Proceedings of the 2005 IEEE/ASME
International Conference on Advanced Intelligent Mechatronics
Monterey, California, USA, 24-28 July, 2005

A Magnetically Controllable Valve to Vary the Resistance of Hydraulic Dampers for Exercise Machines

Brett Levins, Ian Gravagne*

Abstract

While the majority of exercise machines use weights, springs or spinning fans to generate motion resistance, a large number of machines also utilize linear fluid damping. Similar to a shock absorber, linear dampers are compact, extremely reliable, and produce "double positive" resistance (resistance to both directions of motion). However, they are difficult to adjust for higher or lower resistance. This paper illustrates a mechanism to vary the resistance of a linear damper, and illustrates with experimental data certain properties of the damper.

1 Introduction

It has been known for some time that the utilization of linear damping has certain benefits for exercise and exercise machine development (see figure 1). Linear dampers lend a simple and un-intimidating appearance to exercise machines (there are no cables, pulleys, belts or weights, or large spinning wheels), they are often mass produced for the automotive industry and therefore relatively inexpensive, and they are highly efficient at dissipating kinetic energy through heat.

Figure 1: A leg extension machine with a linear hydraulic damper.

*Corresponding author. Address: School of Engineering and Computer Science, MS 97356, Baylor University, Waco, TX, 76798-7356. Email: Ian_Gravagne@baylor.edu.

Their principal drawback, however, is that they are difficult to adjust. Adjustment, if available, usually consists of a valve that must be turned by hand to adjust the size of the gas escape orifice (on pneumatic dampers). Variability is found less commonly on fluid dampers because, unlike pneumatic dampers, fluid cannot escape or be drawn into the damper body, but must be contained within a sealed environment. Linear dampers not based on fluid or gas have been investigated as well [5][9], but without the inertial damping effects of a body of fluid, energy must dissipate through the active elements of the design (e.g. a motor or electromagnet), increasing the size and power consumption, and possibly decreasing the life span, of the device.

There are two principal methods that have been used to adjust the resistance of fluid dampers. The first is simple orifice constriction. For example, when compressing the damper, fluid is pushed out of the main damper chamber below the piston head, forced through a valve, and then reintroduced into the chamber above the piston. While such a valve can be adjusted by means of a motor or solenoid, the external "plumbing" introduces an undesirable level of complexity and bulkiness to the damper, and also increases the likelihood of a leak. Adjustable externally valved fluid dampers are rarely used on exercise machines. See [8] for a complete treatment of this type of damper.

On the other hand, the second method involves changing the properties of the fluid itself. Most notable in this category are the magneto-rheological dampers. Using magneto-rheological fluid (fluid whose viscous properties change under magnetic fields), a constant fluid orifice may be employed (usually in the piston head itself), with a nearby magnet to vary the fluid resistance. These systems can be conveniently packaged, fully sealed and contained, and feature a high degree of variability and bandwidth. They have been extensively studied and characterized [1][2][4][6][7]. However, magneto-rheological fluids break down over time. We estimate that a typical linear damper in a commercial exercise establish-

0-7803-9046-6/05/$20.00 ©2005 IEEE.

ment must be able to endure approximately 1 million strokes per year, over a desired lifetime of at least 5 years. Modern magneto-rheological fluids are capable of dissipating the total energy imparted to them over this time period, but only because of technical advances that make the fluid prohibitively expensive (significantly greater than $100 US per liter). More basic fluids do not have acceptable life spans.

The design featured in this paper falls into the former category. However, the valve consists of only two moving parts and may be fully integrated into the damper piston head itself. Resistance is modulated by the simple application of current. Cost of the proposed valve is kept low because no motors, gears or bearings are necessary, and because the valve – being fully contained within the damping chamber – does not have to maintain a perfect seal under pressure.

2 Damper Model

Notation:

x	magnetic valve gap
A_{in}	fluid inlet orifice area (constant)
A_{out}	fluid outlet orifice area (constant)
A_p	area of piston head (constant)
$A_{\max}$	max effective fluid orifice area (constant)
$A(x)$	measured effective fluid orifice area
$\hat{A}(x)$	projected effective fluid orifice area
f_{flu}	force of fluid exerted on valve
f_{mag}	magnetic force exerted on valve
f_{gas}	gas accumulator force exerted on piston
ΔP	pressure difference across piston
F	force developed by damper
ρ	fluid mass density (constant)
k	adjustment to Bernoulli's equation (constant)
v_p	velocity of piston
$Q(x)$	stiffness of damper
$Q_{\min}$	minimum stiffness of damper (constant)
$g(x)$	fluid force modulation function

The cylindrical damper is illustrated in figures 2 and 3. It uses a high-pressure gas accumulator to accommodate the additional fluid displacement generated by the piston rod during damper compression. (This is a common configuration [8].) There are two piston heads separated by a distance of approximately 10 cm, each with a Teflon seal. The space between the heads contains two electromagnets, which are allowed to move slightly (and independently) along a central steel rod. When current is applied, the magnetic poles resist each other, pushing the magnets apart. Each piston head has a set of three orifices. The magnets move to close off fluid flow into these orifices, creating

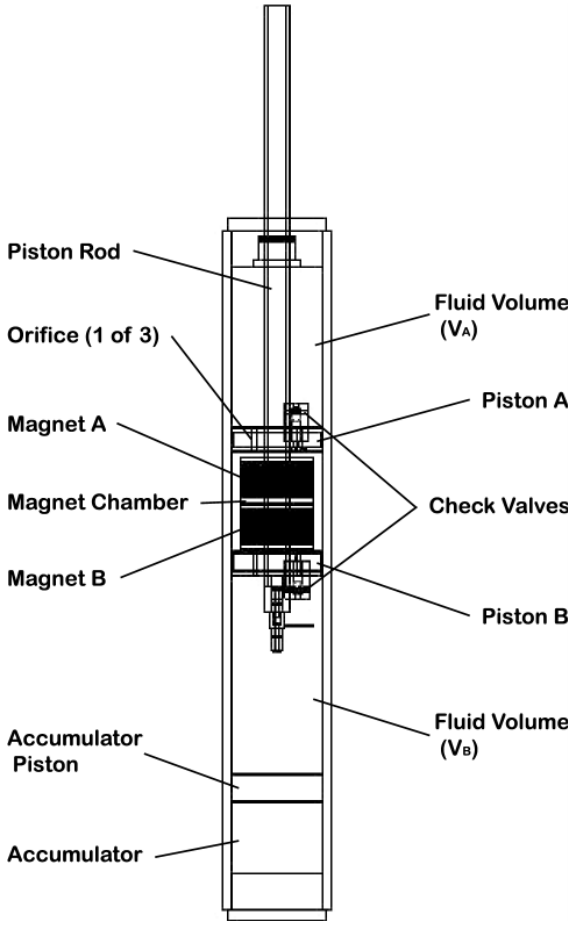

Figure 2: A drawing of the damper cylinder body and valve mechanism.

a small gap between the magnets. We denote the total orifice area of a given piston head A_{in}. During a compression stroke, a pressure difference is generated between fluid volumes V_B and V_A. This static pressure moves magnet B upward, slightly unblocking the inlet orifices and allowing fluid to pass from volume V_B into the magnet chamber between the pistons. On piston A, a one-way check valve with orifice area A_{out} allows fluid to easily escape into volume V_A. The process is reversed during an extension stroke: fluid under pressure pushes magnet A down slightly, opening up a flow path into the magnet chamber. Fluid then passes through a check valve into volume V_B. Higher magnet currents generate higher resistance to flow.

In essence, the magnet blocking the orifice on the high-pressure side of the piston assembly acts as a valve. Once enough static pressure builds to slightly unblock the orifice, the total effective maximum orifice

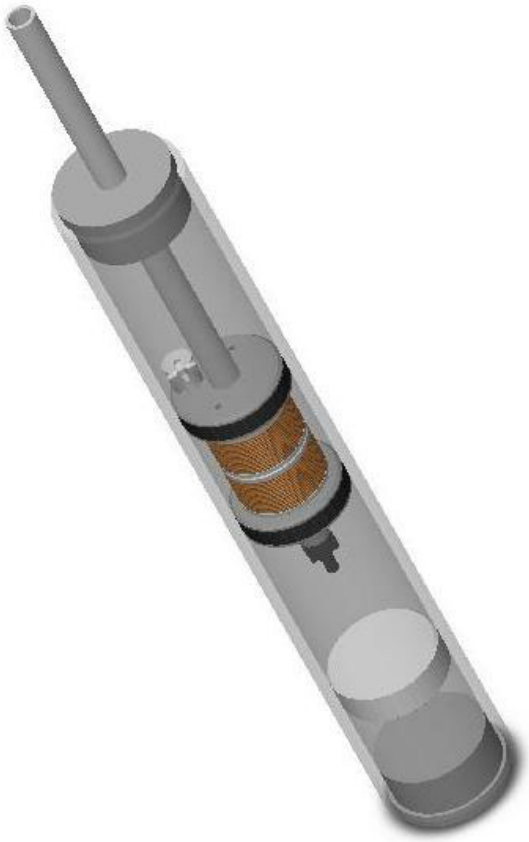

Figure 3: A solid model of the damper showing the piston/magnet assembly.

area $A_{\max}$ is controlled by the force of the opposing magnetic fields. In the experimental damper, each piston head has three orifices of 2.68 mm diameter. The check valve on each piston is 3.22 mm diameter. Thus, $A_{\max}$ consists of 3 inlet areas in "parallel" with each other, and in series with the outlet check valve orifice,

$$\begin{aligned} A_{in} &= 3\pi\left(\frac{2.68}{2}\right)^2; \qquad A_{out} = \pi\left(\frac{3.22}{2}\right)^2 \\ A_{\max} &= \frac{A_{in}A_{out}}{A_{in}+A_{out}} = 5.49mm^2. \end{aligned} \tag{1}$$

Let $x(t)$ be the gap between the piston and the blocking magnet ($0 \le x \le 1.2$ mm), let m be the mass of the magnet and b fluid damping constant. Then the force exerted by the fluid on the magnetic valve f_{flu} must balance the force exerted by the magnetic field, f_{mag}, as

$$m\ddot{x} + b\dot{x} - f_{flu} + f_{mag} = 0. \tag{2}$$

The magnetic force f_{mag} is a function of applied current I. Since the design utilizes the repulsive magnetic force of the two magnets to essentially adjust the orifice area, the force/velocity characteristics of the damper are strictly dependent on the applied current. Because the valve magnet does not have to move very far (less than 1mm) to permit fluid to flow into the magnet chamber, magnets A and B remain in very close proximity. This is beneficial because $f_{mag}(I)$ is then essentially independent of x. The fluid force f_{flu}, however, is a function of the gap x and of the differential pressure across the piston head, $\Delta P = P_B - P_A$. The exact formulation of $f_{flu}(x, \Delta P)$ is complex because it must reflect the transition from a pure reaction force (i.e. when $x = 0$ and force f_{flu} depends only on the pressure) to an impulse force (i.e. when the gap opens and jets of high-velocity fluid impinge on the valve surface, pushing against it). Implicitly, f_{flu} depends on the fluid jet velocity, but the fluid velocity in turn depends on the effective orifice area and the differential pressure. We observe then, that

$$f_{flu} = \Delta P A_{\max} g(x), \tag{3}$$

with with unknown function $g(x) \le 1$.

In the final analysis, we wish to know how the magnet current affects the damper's force vs. velocity relationship. Since the magnetic valve merely changes the effective orifice area, Bernoulli's equation gives the appropriate relationship. Let $A(x)$ be the effective orifice area; note that $A(x) \to A_{\max}$ as $x \to \infty$. Let the piston head area be A_p and assume that the damper push rod diameter is small compared to the piston head itself. Then Bernoulli's equation gives

$$\Delta P = \frac{\rho A_p^2}{2k^2 A(x)^2} v_p^2. \tag{4}$$

Note that the constant k, for true laminar streamline flows, would be $k = 1$; in practice it ranges from 0.8 to 0.9 [3]. The aggregate damper force is just $F = \Delta P A_p$. Two additional effects present themselves as well, the velocity-dependent friction of the piston rod and head sliding past their respective seals, and the (near) constant force exerted by the gas accumulator. Therefore,

$$F_p = \frac{\rho A_p^3}{2k^2 A(x)^2} v_p^2 + c v_p + f_{gas}. \tag{5}$$

Accumulator force f_{gas} also is relatively small compared to the applied force because the piston rod is only 12.7cm in diameter, so the difference in area between piston heads A and B is less than 8%. Thus we assume henceforth that $f_{gas} = 0$. Friction is also a negligible factor here. As seen in figure 4, the force

velocity data for the test cylinder does not exhibit a significant linear component, indicating that $c \simeq 0$ in equation (5).

This paper focuses on the effective orifice area function, $A(x)$. A reasonable hypothesis for $A(x)$ follows by modifying equation (1) to replace A_{in} by a function of the gap x. We assume that the fluid "sees" an orifice that is the surface area of three virtual cylinders, one for each inlet orifice. Each cylinder has radius 1.34mm (half the inlet orifice diameter), with height x. Thus, the total cylinder surface area is $3\times(2\pi\times 1.34x) \simeq 8\pi x$ mm^2. As the gap widens, the cylinder surface area increases linearly, but at some point the limiting orifice area A_{in} is reached and further increases in the valve gap do not yield greater fluid flow (given constant pressure). Then we have the hypothesis function

$$\hat{A}(x) = \frac{\min\{8\pi x, A_{in}\} \times A_{out}}{\min\{8\pi x, A_{in}\} + A_{out}}. \tag{6}$$

Note that $\hat{A}(x) \to A_{\max}$ as $x \to \infty$, suggesting that, as the gap grows significantly larger than the orifice diameter, the gap no longer contricts fluid flow and the orifice itself is the sole flow regulator. The next section gathers experimental evidence to support the hypothesis.

3 Experimental Data

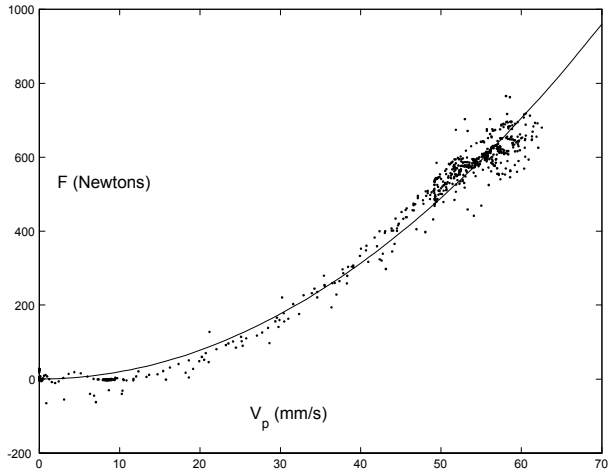

Figure 4: Scatter plot for gap $x = 0.25mm$ during a compression stroke. The solid line is a least-square quadratic fit.

In this section, we want to experimentally examine the function $A(x)$, the effective orifice area. For this purpose, the gap x was fixed at 5 different positions,

$$x \in \{0.25, 0.51, 0.76, 1.02, 1.14\} \text{ millimeters}, \tag{7}$$

and force-velocity scatter plots were obtained using a load cell and linear optical encoder with the damper attached to an exercise machine. See, for example, figure 4. For all 5 gap values, least square error best-fit curves give quadratic stiffness coefficients for equation (5) as

$$Q(x) := \frac{\rho A_p^3}{2k^2 A(x)^2} \in \{195, 136, 116, 117, 116\} \times 10^3. \tag{8}$$

These are plotted versus gap distance in figure 5, which suggests that $Q(x)$ tends asymptotically toward a lower bound, $Q_{\min}$. This can be predicted by remembering that $A(x) \to A_{\max}$ as $x \to \infty$, where $A_{\max}$ is the maximum effective orifice area. The piston head has diameter 47.5 mm, and the hydraulic fluid used in the experiment a mass density of approximately 900 kg/m^3. Using $k = 0.9$ we find that $Q_{\min} = 107.2\times 10^3$. Plotted in figure 5, the predicted value of Q_∞ agrees reasonably well with the asymptotic tendency of the measured estimates of $Q(x)$.

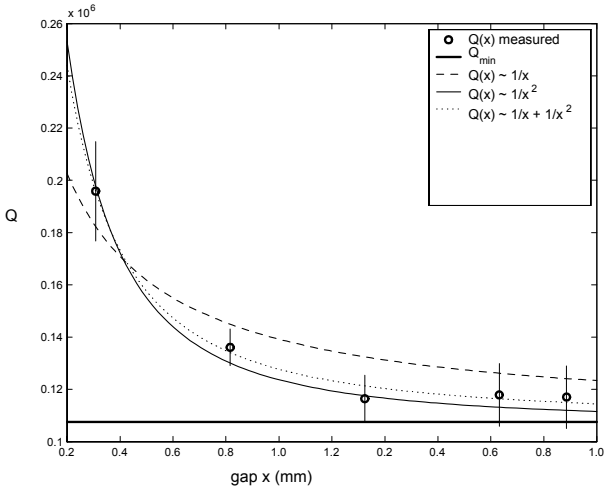

Figure 5: A plot of $Q(x)$, showing measured values and least-square best fit lines. Vertical error bars indicate one standard deviation.

It appears that the values of $Q(x)$ fall nicely around a function of order $\frac{1}{x^2}$; little accuracy is gained by adding a $\frac{1}{x}$ term. The least-square best fit function is $Q(x) = \frac{0.0058}{x^2} + Q_{\min}$. Deriving the valved orifice area function $A(x)$ from equation (8) then gives

$$A(x) = \sqrt{\frac{\rho A_p^3}{2k^2} \frac{x^2}{Q_{\min} x^2 + 0.0058}}. \tag{9}$$

The effective valved orifice area function $A(x)$ is plotted in figure 6 against the hypothesis function, showing the hypothesis function to be fairly accurate in its prediction. Figure 6 also illustrates the fact that only a very small gap is necessary between magnets; in this case, the effective orifice area increases beyond 90% of its maximum within the first 0.5 mm of movement by the valve. (Recall that this permits magnets A and B to be in close proximity, which is desirable since magnetic field strength drops off rapidly as the magnets are separated.)

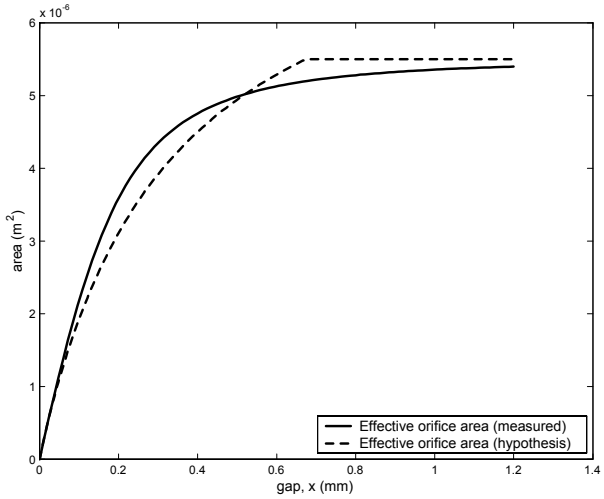

Figure 6: A comparsison of the measured effective orifice area function $A(x)$ and the hypothesis function $\hat{A}(x)$.

In the previous section, we constrained the magnetic valve gap x. Next we permit it to vary, while fixing the current in the magnetic coils. Figure 7 shows the compression and extension strokes for 8 different currents. Best-fit polynomials up to order 2 are plotted to give a representative feel for how the damper resistance varies. (Scatter plot data is omitted for readability.) The plots show that the resistance increases 107% at a speed of 50 mm/s when a current of 2.6 A is applied. The effect is qualitatively striking to the exercise user.

The experimental apparatus is illustrated in figures 8 and 9. Force readings were obtained using a 500 lb. tension/compression load cell (Transducer Techniques SSM-500 with calibrated signal conditioner); linear displacement and velocity measurements were obtained by an externally mounted digital position transducer (Unimeasure LX-EP-15). Wiring for the internal magnets is introduced via a hollow piston rod.

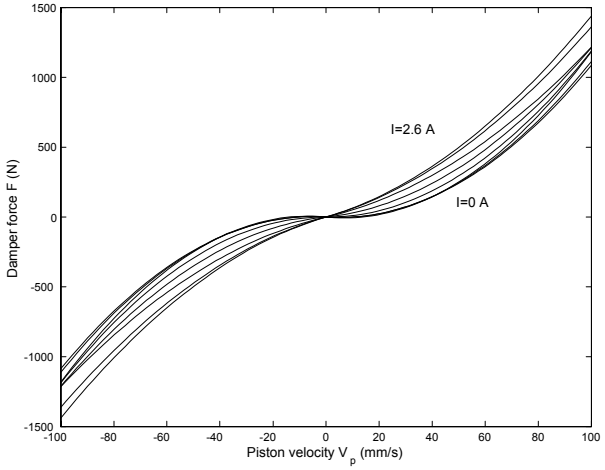

Figure 7: Families of force vs. velocity curves for eight currents spaced approximately evenly from 0 to 2.6 amps.

4 Conclusions

The paper presents a novel magnetically controlled valve to vary the resistance of fluid dampers on exercise machines. The design strives for mechanical simplicity and low cost, and involves only two moving parts. However, design simplicity results in a somewhat complex dynamical model. Experimental data validate the predicted relationship between the valve gap and the effective fluid orifice surface area. This implies that, if the fluid flow rates (or piston velocity) and differential pressure (or damper force) are known, then the gap can be predicted with fair accuracy.

Work is proceeding to more closely examine the system dynamics. The challenge here is to formulate the fluid force f_{flu} exerted on the face of the magnetic valve as a function of the gap and other state variables. When a suitable understanding of this process is reached, we expect to be able to effectively change the damper characteristics via feedback control, if desired. Another phenomenon to investigate is the tendency of the characteristic curves in figure 7 to become more linear with increasing current – a phenomenon not observed in the fixed-gap experiments. (We point out that current research suggests the nonlinear characteristics of the open-loop damper, e.g. figure 4, are beneficial to exercise users.) Further design improvements to the damper are planned, as are more accurate measurements of the characteristics of the damper using a linear dynamometer.

The authors are grateful for a grant from Curves International (contract 097-04-Curves), and for the tech-

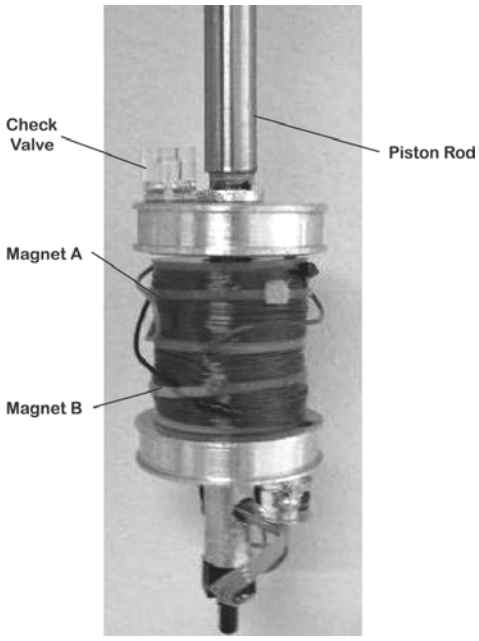

Figure 8: A closeup of the piston/magnet assembly.

nical assistance of Blake Branson.

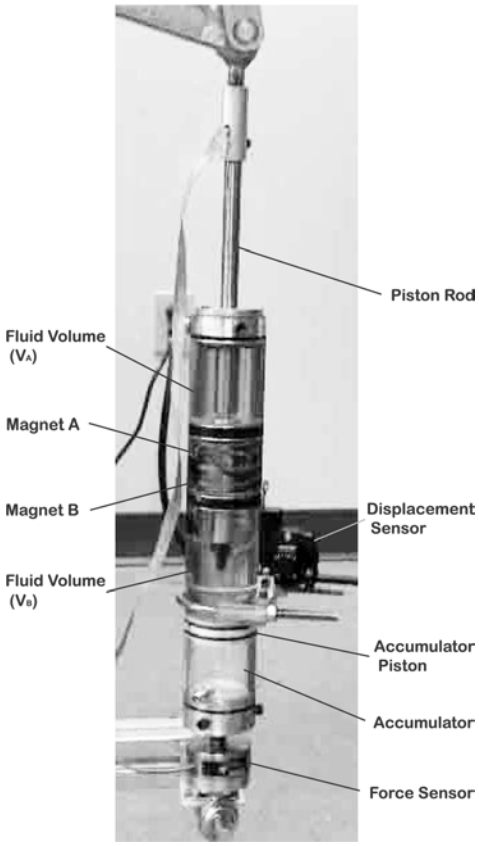

Figure 9: The damper mounted on an exercise machine. The cylinder body is constructed of clear rigid plastic for visibility, and is axially attached to a 500 lb. bidirectional load cell.

References

[1] D. Carlson, D.M. Catanzarite, K.A. St. Clair, "Commercial magneto-rheological fluid devices," Proc. 5th Int. Conf. on ER Fluids, MR Suspensions and Assoc. Tech., Singapore, 1996, pp. 20-28.

[2] M.J. Chrzan, J.D. Carlson, "MR fluid sponge devices and their use in vibration control of washing machines," 8th Annual SPIE Symp. Smart Structures and Materials, Newport Beach, CA, March 2001, pp. 370-378.

[3] J.C. Dixon, The Shock Absorber Handbook, pub. Sept. 1999, Society of Automotive Engineers.

[4] M.R. Jolly, J.W. Bender, J.D. Carlson, "Properties and applications of commercial magnetorheological fluids," J. Intelligent Material Systems and Structures, vol. 10, no. 1, Jan 2000, pp. 5-13.

[5] Y.B. Kim, W.G. Hwang, C.D. Kee, H.B. Yi, "Active vibration control of a suspension system using an electromagnetic damper," Proc. Instn. Mech. Engrs, vol. 215, Part D, pp. 865-873.

[6] J.E. Lindler, Y.T. Choi, N.M. Wereley, "Double adjustable shock absorbers utilizing electrorheological and magnetorheological fluids," Int. J. Vehicle Design, vol. 33, no. 1-3, pp. 189-206.

[7] A. Lukianovich, O. Ashour, W. Thurston, C. Rogers, "Electrically-controlled adjustable-resistance exercise equipment employing magnetorheological fluid," Proc. Soc. Photo-optical and Instrumentation Engrs, vol. 2721, pp. 283-291.

[8] D.J. Purdy, "Theoretical and experimental investigation into an adjustable automotive damper," Proc. Instn. Mech. Engrs, vol. 214, Part D, pp. 265-283.

[9] Y. Suda, T. Shiba, et. al., "Study on electromagnetic damper for automobiles with nonlinear damping force characteristics," Vehicle System Dynamics Supplement, vol. 41, 2004, pp. 637-646.